www.vbripress.com, www.amlett.com, DOI: 10.5185/amlett.2013.fdm.51 Published online by the VBRI press in 2013

Synthesis and electrical properties of $Sr(Bi_{0.5}V_{0.5})O_3$ electroceramic

B. C. Sutar[1], Piyush R. Das[2], R. N. P. Choudhary[2*]

[1]*Department of Physics, Hi-Tech college of Engineering, Bhubaneswar, India*
[2]*Department of Physics, Institute of Technical Education and Research, Siksha 'O' Anusandhan University, Bhubaneswar 751030, India*

[*]Corresponding author. Tel.: (+91) 8763425977; E-mail: crnpfl@gmail.com

Received: 06 January 2013, Revised: 18 March 2013 and Accepted: 17April 2013

ABSTRACT

Lead-free polycrystalline material $Sr(Bi_{0.5}V_{0.5})O_3$ was prepared using a high- temperature solid state reaction technique (calcinations and sintering temperature =850 and 950 ^oC, respectively) using high-purity ingredients. The formation of the material in the monoclinic crystal structure was confirmed by preliminary X-ray structural analysis with room temperature data. The nature of microstructure obtained by scanning electron microscopy (SEM) shows that the compound has well defined grains which are uniformly distributed throughout the surface of the sample. Detailed studies of dielectric and impedance properties of the material carried out in the frequency range of 1 kHz –1MHz at different temperatures (30^0C to 455^0C) have provided many interesting properties. Detailed studies of dielectric properties of the compound showed an existence of diffuse phase transition around 258^0C. The temperature dependence of electrical parameters (impedance, modulus etc.) of the material exhibits a strong correlation of its microstructure with the electrical parameters. The negative temperature coefficient of resistance (NTCR) behavior also was observed in the material. The complex electric modulus analysis indicates the presence of hopping conduction mechanism in the system with non-exponential type of conductivity relaxation. The nature of variation of dc conductivity with temperature confirms the Arrhenius behavior of the material. The ac conductivity spectra show a typical signature of an ionic conducting system, and are found to obey Jonscher's universal power law.

Keywords: Electroceramics; impedance analysis; X-ray diffraction; electric modulus analysis.

B. C. Sutar did his M.Sc (Physics) from Sambalpur University. He is continuing PhD in Physics (Condense Matter) in S O A University. He is presently working as Assistant Professor in the Department of Physics, Hi-Tech college of Engineering, Bhubaneswar, Orissa. His major field of research is in the area of multiferroics/ferroelectric materials.

P. R. Das was born in Cuttack (Orissa) in 1963. He is a postgraduate (1987) in Physics from Ravenshaw college, Cuttack. He did his PhD in Physics (Condense Matter) from IIT Kharagpur in 2008. He is presently working as Associate Professor in the Department of Physics, Institute of Technical Education & Research (Siksha O Anusandhan University), Bhubaneswar, Orissa. His major field of research is in the area of multiferroics/ferroelectric materials.

R. N. P. Choudhary is one of the pioneer researchers and contributors in the field of ferroelectric, Multiferroic and related advanced materials in India and abroad. He has done Ph. D from University of Edinburgh, U.K. He has been actively engaged in teaching and research for the last 40 years at the institutes of national and international reputes such as National Institute of Technology, Jamshedpur (India), Indian Institute of Technology, Kharagpur

(India). He has successfully completed many research projects. He has guided more than four dozens Ph. D students and published more than 600 research papers in national/international journals. He is the member of editorial board of many national/international journals. He is one of the referees of research schemes from DST and CSIR. At present, he is working as a Professor in Department of Physics, Institute of Technical Education and Research (SOA University) Bhubaneswar (India) and many research scholars are doing their research works under his supervision.

Introduction

Out of a large number of ferroelectric oxides discovered so far, a few only have received a considerable attention because of their applications in solid state devices namely, multilayer capacitors, transducers, actuators, ferroelectric random access memory, pyroelectric sensors, optoelectronic devices, etc **[1]**. Some ferroelectric oxides mostly used for device applications are Pb-based: lead titanate ($PbTiO_3$), lead zirconate titanate $Pb(Zr_xTi_{1-x})O_3$ (PZT) (x=composition), lead lanthanum zirconate titanate $(Pb_{1-x}La_x)(Zr_yT_{1-y})_{1-x/4}O_3$ (PLZT) and lead magnesium

niobate $Pb(Mg,Nb)O_3$ (PMN) **[2-5]**, because of their superior ferroelectric and piezoelectric properties as compared to lead free ferroelectrics. Unfortunately, they are very toxic and hazardous for the environment. Therefore, in the recent years, attempts have been made to replace the Pb-based materials with non-lead for the purpose. The enhancement of various physical properties on substitution of proper cations at the A and/or B sites in perovskite ABO_3 (A=mono-divalent and B=tri-hexavalent ions) have led to provide new materials for suitable devices. Investigation of the electrical properties of these materials is desirable to predict their suitability for electronic devices **[6, 7]**. In complex perovskite, the different relaxation processes are present. It is due to variety of defects appearing in them during their fabrication, which may bring a small departure of the dielectric response from the ideal Debye-behavior of the sample. The assessment of relaxation behavior in the material is through impedance and electric modulus studies. The information about conductivity and its associated relaxation in some complex perovskite yielded through electric modulus analyses **[8–12]**.

Among all the lead-free complex perovskite, strontium bismuth vanadate $Sr(Bi_{0.5}V_{0.5})O_3$ (SBV) with a general formula $A(B'_{0.5}B''_{0.5})O_3$ is one of the promising materials for devices. The literature survey suggests that no attempt has been made to study structural, electrical, dielectric, and impedance properties of $Sr(Bi_{0.5}V_{0.5})O_3$. Therefore, an attempt is made to study structural, dielectric, impedance and transport properties for the material for its possible device applications.

Experimental

The polycrystalline sample of $Sr(Bi_{0.5}V_{0.5})O_3$ was synthesized by a solid state reaction method at high temperatures using high-purity $SrCO_3$ (99%, M/s s.d. Fine chem. Pvt. Ltd., India), Bi_2O_3 and V_2O_5 (99.9%, M/s Loba Chemie Pvt. Ltd., India) in a suitable stoichiometry. These oxides and carbonate were thoroughly mixed first mechanically in an agate-mortar and pestle for 1 h, and thereby wet grinding (in methanol) for 1 h to get homogeneous mixture of the ingredients. This mixture was finally calcined at 850^0C (decided on the basis of repeated firing/mixing) for 4 h in air atmosphere. The formation of the desired compound was checked by preliminary X-ray structural analysis. The calcined powder was then cold pressed into cylindrical pellets of diameter10 mm and thickness 1-2 mm at a pressure of 4×10^6 N/m^2 using a hydraulic press. The polyvinyl alcohol was used as binder which was burnt out during high-temperature sintering. The pellets were then sintered at an optimized temperature (950^0C) and time (4 h) in air atmosphere. At room temperature XRD pattern was recorded by a powder diffractometer (D8 ADV, Bruker, Germany) using CuK_α radiation (λ = 1.5405 A°) in a wide range of Bragg's angles 2θ ($20 \leq 2\theta \leq 80$) with a scanning rate of 2^0/min. The microstructure of the sintered pellet was recorded at room temperature by a scanning electron microscope (SEM) (Model: JOEL JSM 5800). The flat surfaces of the pellet were electroded with air-drying conducting silver paste. After electroding, the pellets were dried at 150^0C for 4 h to remove moisture (if any) and then cooled to room temperature before taking any electrical measurements. The impedance and related parameters were measured as a function of temperature (30 – 455^0C) over a wide range of frequencies (1 kHz – 1MHz) using a computer-controlled phase sensitive meter (PSM LCR 4NL, Model: 1735, UK) with a laboratory-designed and fabricated sample holder and other accessories.

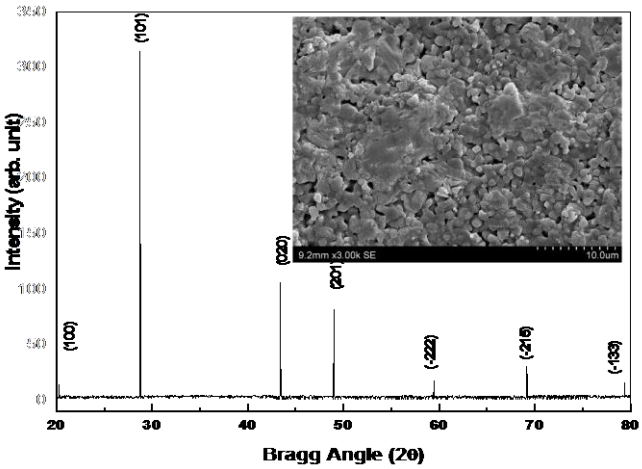

Fig. 1. XRD pattern and SEM (inset) of $Sr(Bi_{0.5}V_{0.5})O_3$ at room temperature.

Table 1. Comparison of d_{obs} and d_{cal} of $Sr(Bi_{0.5}V_{0.5})O_3$ for different hkl plane with intensity ratio.

S. No.	$d_{obs.}$	$d_{cal.}$	I/I_o	h	k	l
1.	4.3708	4.3708	4	1	0	0
2.	3.1025	3.1023	100	1	0	1
3.	2.0832	2.0835	34	0	2	0
4.	1.8574	1.8573	26	2	0	1
5.	1.5534	1.5535	6	-2	2	2
6.	1.3573	1.3574	10	-2	1	5
7.	1.2065	1.2062	5	-1	3	3

Results and discussion

Structural properties

Fig. 1 shows the XRD pattern of $Sr(Bi_{0.5}V_{0.5})O_3$ at room temperature. The diffraction peaks of the compound were indexed in the different crystal systems and unit cell configurations using a standard computer program package ''POWD'' **[13]**. A monoclinic unit cell was selected on the basis of good agreement between observed and calculated inter planar spacing d (i.e., $\sum\Delta d = d_{obs} - d_{cal}$ = minimum). The lattice parameters of the selected unit cell were refined using the least-squares sub-routine of the standard computer program package POWD. The refined lattice parameters are; a = 4.818(6) Å, b = 4.167(6) Å, c = 7.331(6) Å, β = 114.88^0 and V=133.52 Å^3. Using refined lattice parameters, each peak was indexed and inter-planar

spacing (d) of reflection planes of the compound was calculated, and compared with its observed value (**Table 1**).

The crystallite size (P) of the sample was calculated using Scherrer equation: $P = k\lambda/(\beta_{1/2}\text{Cos}\theta)$, where k = 0.89, λ = 1.5405Å and $\beta_{1/2}$ = broadening of peak at half the wavelength (FWHM). The average value of P was found to be 136 nm. As the powder sample was used to get XRD pattern, contributions of strain and other effects in the broadening of XRD peaks and crystallite size calculation have been ignored. The SEM micrograph of sintered pellet at room temperature is shown in **Fig. 1** (inset). The SEM micrograph shows the polycrystalline nature of Material where the grains of different sizes and shapes are in-homogeneously distributed throughout the sample surface. The grains are densely and closely packed with a few scattered pores with a certain degree of porosity. The grain size lies in the range of 1-4 μm.

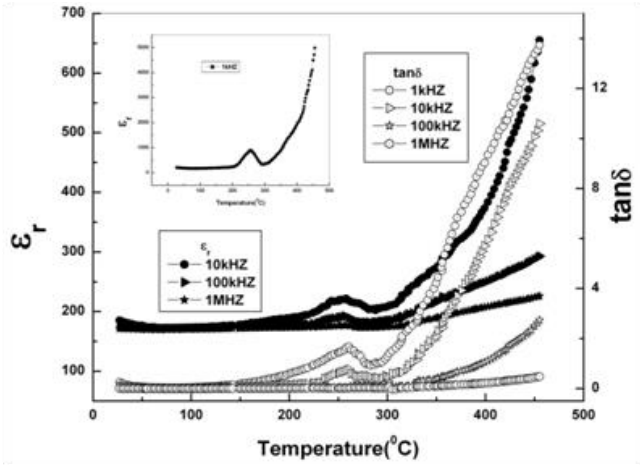

Fig. 2. Temperature dependency of (a) ε_r and (b) tanδ at different frequencies of $Sr(Bi_{0.5}V_{0.5})O_3$.

Dielectric properties

Fig. 2 shows the temperature dependence of relative dielectric constant (ε_r) and loss tangent (tanδ) of $Sr(Bi_{0.5}V_{0.5})O_3$ with temperature at different frequencies. It is also observed that both ε_r and tanδ decrease on increasing frequency, which is a general feature of dielectric materials **[14]**. Again, ε_r increases gradually on further increasing of temperature to its maximum value (ε_{max}) and then decreases. The dielectric anomaly observed around 258^{0}C may be due to the phase transition. Above this anomaly further increase of ε_r (at lower frequency) may be considered due to space charge polarization which comes from mobility of ions and imperfections in the material. These combined effects produce a sharp increase in the relative dielectric constant on increasing temperature. Similar trend of variation is observed in tanδ (as in ε_r) as a function of temperature. The rate of increase in tanδ in the material at low temperature is slow, whereas at higher temperature the increase is relatively sharp. This sharp increase in tanδ at higher temperatures may be due to scattering of thermally activated charge carriers and presence of some unknown defects including oxygen vacancies in the sample. At higher temperatures the conductivity begins to dominate, which in turn, is responsible for rise in tanδ. At the same time, the defect structure along with the presence of V^{5+} ions accounts for its high temperature ferroelectrics **[15-17]**. The higher value of tanδ at high temperature may be due to space charge polarization and ferroelectric domain wall contribution.

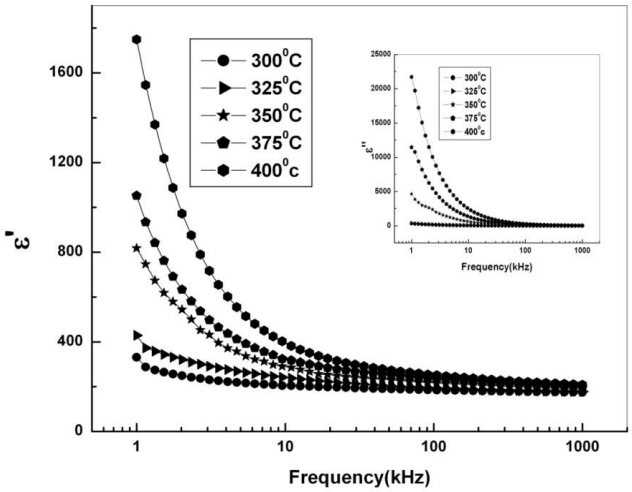

Fig. 3. Variation of ε' and ε'' with frequency at different temperatures of $Sr(Bi_{0.5}V_{0.5})O_3$.

In order to examine the effect of space charge polarization in low frequency range and at high temperatures, we have plotted the real and imaginary part of dielectric constant (i.e., ε′, ε″) with frequency at different temperatures. Figure 3 shows the variation of ε′ and ε″ with frequency above 300 ^{0}C. There is a sharp decrease in value of ε′ and ε″ in the lower frequency region and showing a frequency independent value of these parameters in the high frequency region. The strong decrease of real and imaginary part of dielectric constant towards low frequency range may be due to space charge polarization and interface effect.

Impedance spectrum analysis

Impedance spectroscopy (IS) **[18]** is the most reliable and important technique to study the electrical properties and process of the materials. The IS technique is based on analyzing the ac response of a system to a sinusoidal perturbation, and subsequent calculation of impedance and related parameters as a function of frequency of the perturbation at different temperatures **[19-22]**. A parallel resistance and capacitance circuit corresponding to equivalent to the individual component of the materials (i.e., bulk and grain boundary) represents a semicircle. Impedance data of materials (i.e., capacitive and resistive components), represented in the Nyquist plot, lead to a succession of semicircle. The frequency dependence of dielectric properties of the materials is normally described in terms of complex dielectric constant (ε^*), complex impedance (Z*), electric modulus (M*) and dielectric loss ($\tan\delta$) and are related to each other as

$$Z^* = Z' - jZ'' = R_s - \frac{j}{\omega c_s}$$

$$\varepsilon^* = \varepsilon' - j\varepsilon''$$

$$M^* = M' + jM'' = j\omega Co Z^*_{\omega}$$

$$\tan\delta = \frac{\varepsilon''}{\varepsilon'} = \frac{Z'}{Z''} = \frac{M''}{M'}$$

where ω is the angular frequency, ε_0 is the permittivity in free space, R_s and C_s are resistance and capacitance in series respectively. The above expressions offer a wide scope for graphical representation as they can be used to calculate complex impedance of the electrode/ceramic/electrode capacitor (demonstrated as the sum of the single RC circuit with parallel combination) as per the relation reported by our earlier paper **[23]**. **Fig. 4** shows the variation of real part of impedance (Z') with frequency at different temperatures. The values of Z' decrease with rise in frequency and temperature.

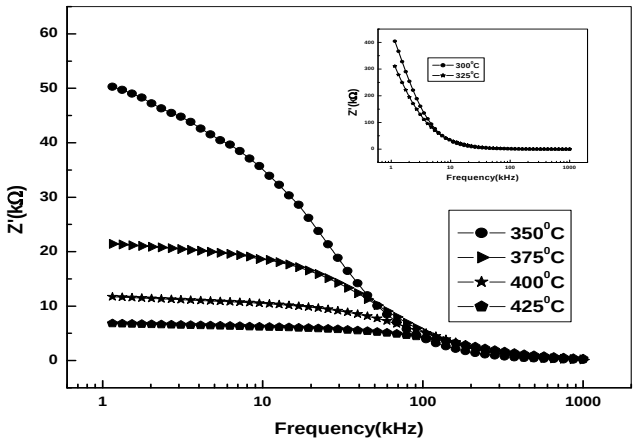

Fig. 4. Variation of Z' with frequency at different temperatures of $Sr(Bi_{0.5}V_{0.5})O_3$.

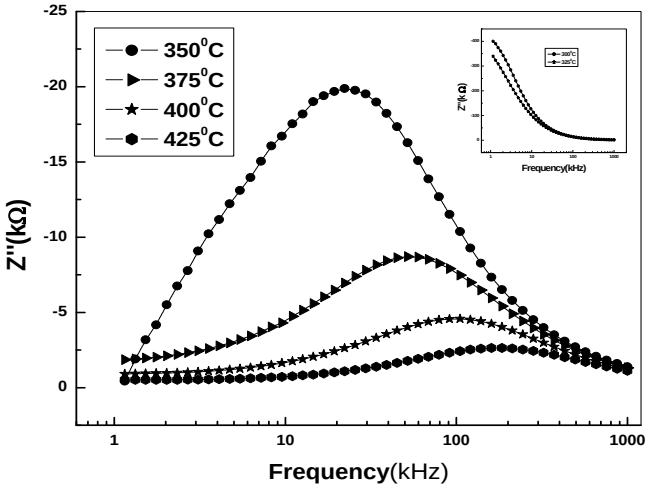

Fig. 5. Variation of Z'' with frequency at different temperatures of $Sr(Bi_{0.5}V_{0.5})O_3$.

Z' decreases on increasing temperature in the low-frequency region, and merges in the high-frequency region irrespective of temperature. This nature may be due to the release of space charge **[14]**. The reduction in barrier properties of the materials with rise in temperature may be a responsible factor for enhancement of ac conductivity of the materials at higher frequencies **[24, 25]**. Further, in the low frequency region, there is a decrease in magnitude of Z' with rise in temperature showing negative temperature coefficient of resistance (NTCR) behavior. This behavior is changed drastically in the high frequency region showing complete merger of Z' plot above a certain fixed frequency. At high frequency Z' value of each temperature coincides implying the possible release of space charge **[26]**. At a particular frequency Z' becomes independent of frequency and shift towards the higher frequency side (with rise in temperature). The shift in Z' plateau indicates the existence of frequency relaxation process in the material. The curves display single relaxation process and indicate the increase in ac conductivity with increase in temperature and frequency **[27]**. **Fig. 5** shows the variation of Z'' with frequency at different temperatures. The variation of Z'' with frequency attains a maximum value at a particular frequency known as electrical relaxation frequency (ω_{max}).

This feature becomes noticeable on and above 350^0C but below this temperature there is a monotonous decrease in Z'' with frequency. It is observed that the peaks are shifted towards higher frequencies side on increasing temperature. The change in the (a) peak position and (b) broadening on increasing/decreasing temperature exhibits the presence of temperature dependence of relaxation processes in the compound. The Z''_{max} shifts to higher frequency side on increasing temperature indicate the increase of tangent loss in the samples. The relaxation process may be due to the presence of electrons / immobile species at low temperatures and defects / vacancies at higher temperatures. The asymmetric broadening of the peaks suggests a spread of relaxation time with two equilibrium positions. The peak heights are proportional to bulk resistance (R_b), and can be explained by the equation;

$$Z''[= R_b\{\omega\tau/(1+\omega^2\tau^2)\}]$$

Further, the magnitude of Z'' decreases gradually with a shift in peak frequency towards high frequency side, and it finally merges in the high frequency region. This is an indication of the accumulation of space charge in the material **[23]**. **Fig. 6** shows the complex impedance spectrum (Nyquist-plot) of $Sr(Bi_{0.5}V_{0.5})O_3$ at selected temperatures. Only one semicircular arc is observed at low temperatures that represents the contribution of the grains (bulk) in the impedance. Above 350^0C, there is a trend to form a semicircular, and finally a semicircular arc is formed on increasing temperature. The presence of a single semicircular arc is due to the bulk property of the material. At higher temperatures (>375^0C) the plot can be characterized by the presence of two overlapping semicircular arcs with their centers lying below the real axis. The high-frequency semicircle could be attributed to the bulk (grain) property of the material. The low-frequency arc of the impedance spectrum (at elevated temperatures) has been attributed to the presence of grain boundary. It suggests the departure from ideal Debye behavior and justifies the presence of a constant phase

element (CPE) **[28]** in fitting of the circuit. The CPE admittance is generally represented as $Y(\text{CPE}) = A_0(j\omega)^n = A\omega^n + jB\omega^n$, **[22]** where $A = A_0\text{Cos}(n\pi/2)$ and $B = A_0\text{Sin}(n\pi/2)$. A_0 and n are frequency independent but temperature dependent parameters, A_0 determines the magnitude of the dispersion and n varies between zero and one. The CPE describes an ideal capacitor and resistor for $n = 1$ and 0 respectively **[25, 26]**. The equivalent circuit for the observed two overlapping semicircle arcs of the impedance spectrum can be modeled by a series array of parallel combination of (i)a resistance (bulk resistance), capacitance (bulk capacitance) and a CPE, with another parallel combination of (ii) a resistance (grain boundary resistance), capacitance (grain boundary capacitance) as shown in **Fig. 6**. The electrical process at these temperatures may be considered due to intra-grain phenomenon.

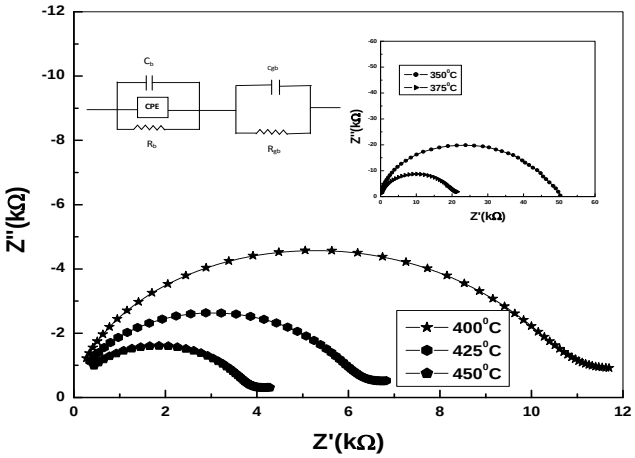

Fig. 6. Nyquist plot and equivalent circuit of $Sr(Bi_{0.5}V_{0.5})O_3$.

Complex electric modulus analysis

The electrical modulus analysis is very useful to detect electrode polarization, grain boundary conduction effect, bulk properties, electrical conductivity and relaxation time **[32, 33]**. This technique also provides an insight into the electrical processes occuring in the materials at different temperatures and frequencies. The following relations of electrical modulus are normally used to estimate M' and M''

$$M' = A\left[\frac{(\omega RC)^2}{1+(\omega RC)^2}\right] = A\left[\frac{\omega^2\tau^2}{1+\omega^2\tau^2}\right]$$

$$M'' = A\left[\frac{\omega RC}{1+(\omega RC)^2}\right] = A\left[\frac{\omega\tau}{1+\omega^2\tau^2}\right]$$

where $A = \frac{C_o}{C}$ Using the above formalism the inhomogeneous nature of polycrystalline ceramics with bulk and grain boundary effects can easily be probed, which cannot be distinguished from complex impedance plots. The other major advantage of the electric modulus formalism is to suppress the electrode effect.

Fig. 7 shows the variation of M' and M'' with frequency at selected high temperatures (>350^{0}C). The value of M' approaches to zero on lowering frequency with monotonic dispersion, whereas the values of M' coincide on further rise in temperature and frequency.

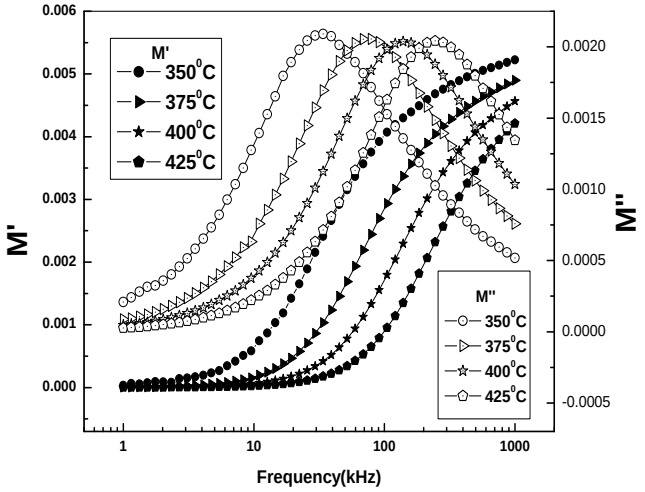

Fig. 7. Variation of M' and M'' with frequency at different temperatures of $Sr(Bi_{0.5}V_{0.5})O_3$.

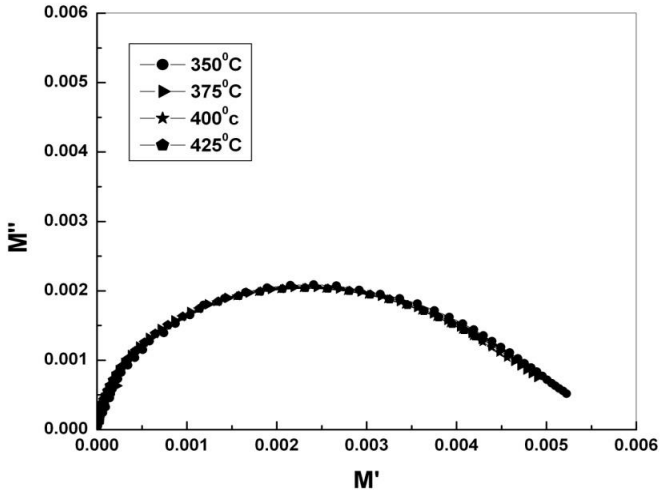

Fig. 8. Variation of M' and M'' of $Sr(Bi_{0.5}V_{0.5})O_3$ at different temperatures.

This may be due to presence of conduction phenomenon and short range mobility of charge carriers. This implies that there is a lack of restoring force for flow of charges under the influence of steady electric field **[29-32]**. The M''_{max} peak shifts to higher frequency side. This nature of dielectric relaxation suggests that the hopping mechanism of charge carriers dominates intrinsically at higher temperatures in thermally activated process. Asymmetric broadening of the peak indicates spread of relaxation with different time constants, which suggests occurrence of non-Debye type relaxatation **[33]**.

Complex modulus spectrum of $Sr(Bi_{0.5}V_{0.5})O_3$ at selected temperatures is shown in **Fig. 8**. The appearance of asymmetric semicircular arcs in the complex impedance plots is confirmed by this method. This indicates that electrical relaxation phenomenon occurs in the above

material. It is clear that the modulus plane shows a single semicircle. The intercept on the real axis indicates the total capacitance contributed by the grain and grain boundaries. It is confirmed in our M" versus frequency plot where the grain boundaries are negligible. Even if present, their contribution to the overall capacitance of the material is very small, and does not affect the relaxation process much. The modulus spectrum shows a marked change in its shape/size with rise in temperature suggesting a probable change in the capacitance value of the material as a function of temperature.

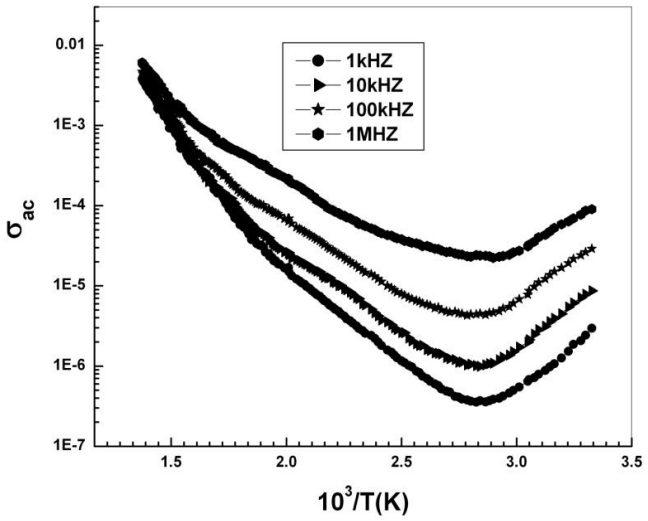

Fig. 9. Variation of σ_{ac} with inverse of absolute temperature of $Sr(Bi_{0.5}V_{0.5})O_3$ at different frequencies.

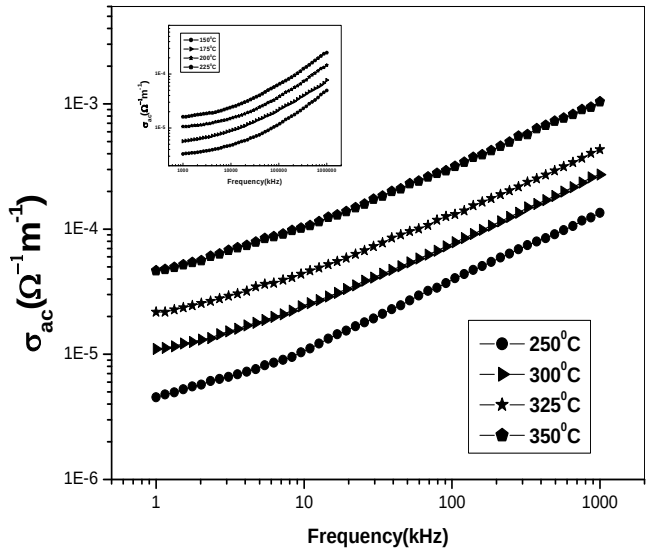

Fig. 10. Variation of σ_{ac} with frequency at different temperatures of $Sr(Bi_{0.5}V_{0.5})O_3$.

AC conductivity analysis

The temperature dependence of ac conductivity at different frequencies (**Fig. 9**) can be calculated from the dielectric data using the relation: $\sigma_{ac} = \omega\varepsilon_r\varepsilon_0\tan\delta$, where ε_0 = dielectric permittivity of free space and other parameters have their usual meanings. The activation energy E_a (which is dependent on a thermally activated process) can be calculated using an empirical relation: $\sigma_{ac} = \sigma_0 \exp(-E_a/kT)$, where k = Boltzmann constant and σ_0 = pre-exponential factor. For each frequency in the plot, occurrences of different slopes at different temperature regions suggest the presence of multiple conduction processes in the sample with different activation energy **[34]**. The frequency dependence of conductivity of the material (**Fig. 10**) can be explained by Jonscher's power law by the equation; $\sigma_{ac} = \sigma_{dc} + A\omega^n$, where σ_{dc} is the dc conductivity (frequency independent plateau in the low frequency region), A is the temperature dependent frequency pre-exponential factor and n is the power law exponent.

The value of n varies from 0 to 1 depending on temperature **[35]**. The exponent n represents the degree of interaction between the mobile ions with the lattices around them **[31]**. The low frequency dispersion attributes to the ac conductivity whereas the frequency independent plateau region of the conductivity pattern corresponds to dc conductivity of the material. The temperature at which grain resistance dominates over grain boundary resistance is marked by a change in slope of ac conductivity with frequency. The frequency at which the change of slope takes place is known as the hoping frequency. It corresponds to polarons hopping of charged species. The hopping frequency shifts to higher frequency side on increasing temperature.

Conclusion

The polycrystalline sample of $Sr(Bi_{0.5}V_{0.5})O_3$ was prepared by a high-temperature solid-state reaction technique. X-ray analysis exhibits the monoclinic crystal structure of the compound at room temperature. The surface morphology of the compound, studied by SEM, gives is overall dense and closely packed with irregular grains of different grain sizes in the range of 1-4 µm. The complex impedance plots reveal the contribution of both bulk and grain boundary effects. Due to low loss the quality factor of the material is high which can be used in many applications including microwaves. The complex electrical modulus analysis indicated non-exponential type of conductivity relaxation in the material. The frequency dependence of ac conductivity obeys Jonscher's universal power law.

Reference

1. Haertling G H *J. Am. Ceram. Soc.* **1999**, 82, 797–818. **DOI:** 10.1111/j.1151-2916.1999.tb01840.x
2. Lines,M.E. , Glass, A.M. Principle and Application of ferroelectrics and Related Materials (Clarndon Press, Oxford, **1977**)
3. Selvamani R, Singh G, Sathe V, Tiwari V S and Gupta P K *J. Phys.: Condens. Matter.*2011, 23,055901. **DOI:** 10.1088/0953-8984/23/5/055901
4. Kingon,A.I ,Terblanché,P.J,Clark, J.B. *Materials* Science *and Engineering*. **1985**,71,391. **DOI:**10.1016/0025-5416(85)90258-7
5. Shvartsman,V.V., Dec, J. , Kukasiewicz,T., Kholkin, A.L., Kleemann,W.K. *Ferroelectrics* **.2008**,373,77. **DOI:** 10.1080/00150190802408739
6. Zhao,Shixi.,Li,Qiang.,Feng,Yuchuan.,Nan, Cewen. *Journal of Physics and Chemistry of Solids.* **2009** *,70,* 639. **DOI:** 10.1016/j.jpcs.2009.01.009
7. Yasuda,N.,Ueda,Y.*J.Phys.:Condens.Matter*.**1989**,1,497. **DOI:** 10.1088/0953-8984/1/2/020
8. Darlington, C.N.W. *J. Phys.: Condens. Matter* .**1991**,3 ,4173.

DOI: 10.1088/0953-8984/3/23/006
9. Lampis, N., Sciau, P., Lehmann, A.G. *J. Phys.: Condens. Matter.* **1999**,11, 3489. **DOI:** 10.1088/0953-8984/11/17/307
10. Lvanov, S.A., Tellgren,R., Rundlof, H., Thomas, N.W., Ananta, S. *J. Phys.: Condens. Matter.***2000**, 12, 2393. **DOI:** 10.1088/0953-8984/12/11/305
11. Bonny, V., Bonin, M., Sciau, P., Schenk, K.J., Chapuis, G., *Solid State Commun.* **1997**, 102, 347. **DOI:** 10.1016/S0038-1098(97)00022-7
12. Mishra,Amodini.,Choudhary,S.N.,Prasad,K.,Choudhary,R.N.P.,*PhysicaB*.**2011**,406,3279. **DOI:** 10.1016/j.physb.2011.05.040
13. POWD,E.Wu,an interactive powder diffraction data interpretation and indexing program, Ver. 2.1, School of Physical Sciences, Flinders University South Bedford Park, SA 5042 Australia.
14. Anderson,J.C. Dielectrics (Chapman & Hall, London, **1964**).
15. Pradhan,D.K,Behera,B.,Das,P.R.*J.Mater.Scie:MaterElectron*.**2012**,23,779. **DOI:** 10.1007/s10854-011-0492-9
16. Barick,B.K,Mishra,K.K,Arora,A.K,Choudhary,R.N.P,Pradhan,Dillip .K.*J.Phys.D.Appl.Phys*.**2011**,44,355402. **DOI:** 10.1088/0022-3727/44/35/355402
17. Sutar,B.C.,Pati.B,Parida.B.N.,Das,Piyush.R.,Choudhary.R.N.P.*J.Mater.Scie:MaterElectron*.**2012**. **DOI:** 10.1007/s10854-012-1054-5.
18. Macdonald, J. R. Impedance Spectroscopy Emphasizing Solid Materials and Systems, (Wiley, New York, **1987**).
19. Sen,S.,Choudhary,R.N.P.*Mater.Chem.Phys*.**2004**,87,25646. **DOI:** 10.1016/j.matchemphys.2004.03.005.
20. Brahma,S.,Choudhary,R.N.P.,Thakur,A.K.,*PhysicaB*.**2005**,355,188. **DOI:** 10.1016/j.physb.2004.10.091.
21. Suchanicz,J.,*Mater.Sci.Eng.B*.**1998**,55,114. **DOI:** 10.1016/S0921-5107(98)00188-3.
22. Suman,C.K.,Prasad,K.,Choudhary,R.N.P.*J.Mater.Sci*.**2006**,41,369. **DOI:** 10.1007/s10853-005-2620-5.
23. Das,P.R.,Pati,B.,Sutar,B.C.,Choudhary,R.N.P.*Adv.Mater.Lett*.**2012**,3(1),8. **DOI:** 10.5185/amlett.2011.4252.
24. Provenzano, V., Boesch, L.P., Volterra, V., Moynihan, C.T., Macedo, P.B., *J. Am. Ceram.Soc*.**1972**,55,492. **DOI:** 10.1111/j.1151-2916.1972.tb13413.x.
25. Jain, H., Hsieh, C.H., *J. Non-Cryst. Solids*, **1994**,172-174, 1408 .
26. Suman,C.K.,Prasad,K.,Choudhary,R.N.P.,*J.Mater.Sci*.**2006**,41,369. **DOI:** 10.1007/s10853-005-2620-5.
27. Chatterjee, S., Mahapatra, P.K., Choudhary, R.N.P., Thakur, A.K. *Phys. Stat. Sol.(a)*.**2004**,201,588. **DOI:** 10.1002/pssa.200306741.
28. Pradhan,DK., Choudhary,R N P., Rinaldi ,C .and Katiyar ,R S .*J. Appl. Phys.* **2009**.106, 024102. **DOI:** 10.1063/1.3158121.
29. Jonscher, A.K.*Nature*.**1977**,267,673. **DOI:** 10.1038/267673a0.
30. Sen,S.,Choudhary,R.N.P,andPramanik,P.*Phys.B.***2007**,387,56 **DOI:** 10.1016/j.physb.2006.03.028.
31. Pati,Biswajit.,Sutar,B.C.,Parida,B.N.,Das,P.R.,Choudhary,R.N.P.*J. Mater.Sci:Mater Electron*.**2012**. **DOI:** 10.1007/s10854-012-0983-3
32. Hodge,I.M.,Ingram,M.D.andWest,A.R.,*J.Electroanal.Chem*.**1975**,58 ,429. **DOI:** 10.1016/S0022-0728(75)80102-1 .
33. Macdonald,JR.*SolidstateIonics*.**1984,**13. **DOI:** 10.1016/0167-2738(84)90049-3.
34. Choudhary, R.N.P., Pradhan, D.K. , Tirado, C.M. , Bonilla, G.E., Katiyar,R.S. *J. Mater. Sci*.**2007**,42,7423. **DOI:** 10.1007/s10853-007-1835-z.
35. Jonscher,A.K. Dielectric Relaxation in Solids (Chelsea Dielectric Press, London, **1983**).

